Published in final edited form as:
Dev Biol. 2009 March 15; 327(2): 339–351. doi:10.1016/j.ydbio.2008.12.016.

Identification and subclassification of new *Atoh1* derived cell populations during mouse spinal cord development

George R. Miesegaes[1], **Tiemo J. Klisch**[3], **Christina Thaller**[2], **Kaashif A. Ahmad**[3], **Richard C. Atkinson**[3], and **Huda Y. Zoghbi**[1,3,4,5,6,*]

[1]Program in Cell and Molecular Biology, Baylor College of Medicine, Houston Tx 77030

[2]Verna and Marrs McLean Department of Biochemistry and Molecular Biology, Baylor College of Medicine, Houston Tx 77030

[3]Departments of Molecular and Human Genetics, Baylor College of Medicine, Houston Tx 77030

[4]Department of Pediatrics, Baylor College of Medicine, Houston Tx 77030

[5]Departments of Neurology, and Neuroscience, Baylor College of Medicine, Houston Tx 77030

[6]Department of Howard Hughes Medical Institute, Baylor College of Medicine, Houston Tx 77030

Summary

At spinal levels, sensory information pertaining to body positioning (proprioception) is relayed to the cerebellum by the spinocerebellar tract (SCT). In the past we revealed the basic helix-loop-helix transcription factor *Atoh1* (*Math1*) to be important for establishing Dorsal Progenitor 1 (DP1) commissural interneurons, which comprise a subset of proprioceptive interneurons. Given there exists multiple subdivisions of the SCT we asked whether *Atoh1* may also play a role in specifying other cell types in the spinal cord. Here, we reveal the generation of at least three DP1 derived interneuron populations that reside at spatially restricted positions along the rostral-caudal axis. Each of these cell populations express distinct markers and anatomically coincide with the cell bodies of the various subdivisions of the SCT. In addition, we found that as development proceeds (e.g. by E13.5) *Atoh1* expression becomes apparent in the dorsal midline in the region of the roof plate (RP). Interestingly, we find that cells derived from *Atoh1* expressing RP progenitors express SSEA-1, and in the absence of *Atoh1* these progenitors become SOX9 positive. Altogether we reveal the existence of multiple *Atoh1* dependent cell types in the spinal cord, and uncover a novel progenitor domain that arises late in development.

Keywords

Proprioception; Roof plate; Spinal cord development; Dorsal interneuron; *Math1*; Mouse; *Atoh1*

Introduction

The ability to acquire and maintain a neural representation of one's physical boundaries in three-dimensional space, independent of visual cues, is the underlying principle behind the phenomenon known as proprioception. Originally characterized over one hundred years ago (Sherrington, 1906), the proprioceptive system carries information pertaining to body

*Author for correspondence: Huda Y. Zoghbi, M.D., Investigator, Howard Hughes Medical Institute, Professor, Departments of Pediatrics, Neurology, Neuroscience, and Molecular and Human Genetics, Neurology, Neuroscience, and Molecular and Human Genetics, Baylor College of Medicine, T807, One Baylor Plaza, Mail Stop 225, Houston, Texas 77030, hzoghbi@bcm.tmc.edu.

positioning, balance, posture, and fine motor control to higher brain centers primarily in an unconscious fashion. In humans, case studies of individuals with proprioceptive damage have been well documented and clearly demonstrate its importance in allowing and coordinating even the most basic physical movements (Cole and Paillard, 1995; Paillard, 1999).

During mouse development, many of the cell types involved in proprioception are specified by *Atonal homolog 1* (*Atoh1*, originally *Math1*), a member of the basic-Helix-Loop-Helix (bHLH) family of transcription factors. In the hindbrain, *Atoh1*-expressing progenitors in the rhombic lip give rise to cerebellar granule cells, a subset of deep cerebellar nuclei, the ventral cochlear nucleus, cells in the medial and lateral vestibular nucleus, and the precerebellar nuclei (Machold and Fishell, 2005; Wang et al., 2005). These progenitors either fail to divide or are not generated in *Atoh1* null mice (Ben-Arie et al., 1997). In the inner ear, *Atoh1* is expressed in epithelial progenitors that generate hair cells and is critical for both auditory and vestibular hair cell specification (Bermingham et al., 1999), and is also expressed in Merkel cells and a subset of joint chondrocytes (Ben-Arie et al., 2000) although its role in these cell types remains elusive. In the spinal cord, *Atoh1* specifies a subset of dorsally derived interneurons that populate the intermediate gray and serve as commissural interneurons of the spinocerebellar tracts (Bermingham et al., 2001; Helms and Johnson, 1998).

Physiological and anatomical studies together with recently acquired genetic data have provided mechanistic insight into the generation and function of dorsal interneurons in vivo. Currently, a total of six dorsal interneuron progenitor domains (DP1-DP6) have been identified from which at least eight cell types are produced (Lee et al., 2000; Millonig et al., 2000; Muller et al., 2002; Muroyama et al., 2002). The DP1-DP3 domains can be identified by the unique expression of the bHLH transcriptional activators *Atoh1*, *Ngn1*, and *Mash1*, respectively (Gowan et al., 2001). Since these factors are downregulated upon differentiation, it is believed that subtype identity is maintained postmitotically through the combinatorial expression of various LIM-homeodomain transcription factors, as was previously demonstrated in the ventral spinal cord (Briscoe et al., 2000). In this regard, *Atoh1*-defined DP1 progenitors give rise to *Lhx2* and *Lhx9* expressing cells (Bermingham et al., 2001; Gowan et al., 2001; Lee et al., 1998), *Ngn1*-defined DP2 progenitors give rise to *Lhx1*, *Lhx5*, and *FoxD3*-expressing cells, and DP3 progenitors generate *Isl1*-expressing cells (Gross et al., 2002). Dorsally derived precursors go through a transitory phase along the lateral margin of the neuroepithelium known as the sojourn zone, prior to arriving at their final destination (Altman and Bayer, 2001). DP1-DP3 progenitors arise between E9.5–E10.5 whereas their corresponding postmitotic migratory precursors are observed between E10.5–E11.5 (Helms and Johnson, 2003).

Pulse-chase labeling studies in developing rat embryos revealed that vertically oriented commissural interneurons arise from progenitors located in the dorsal neuroepithelium, and moreover, are detected in the intermediate gray at a time corresponding to E11.5 in mouse (Altman and Bayer, 1984; Nandi et al., 1991). However, 24 h later a second population is observed migrating laterally upon entering the intermediate gray that is not commissural in nature and is horizontally oriented; distinct banding patterns of perpendicularly-oriented axon bundles (termed microsegments) were observed (Altman and Bayer, 1984; Nandi et al., 1991). It was proposed in rat that the vertically oriented commissural interneurons were born prior to E14 (E12 in mouse) whereas the horizontally-oriented, ipsilaterally-projecting interneurons were likely born thereafter (Altman and Bayer, 2001). On a separate but related issue, it is worth noting that past studies serving to map the trajectories of proprioceptive afferents revealed significant innervation within the intermediate gray (Ishizuka et al., 1979; Scheibel and Scheibel, 1969).

Many questions remain with regard to the role of *Atoh1* throughout spinal cord development. For example, it has yet to be addressed which, if any, dorsal progenitor domains give rise to

ipsilaterally projecting interneurons. Using a transgenic mouse model that expresses *tau*-GFP under the control of an *Atoh1enhancer* region, Imondi et al. identified a DI1 neuronal subpopulation, which gives rise to isilateral projections to the lateral funiculus but it has yet to be demonstrated that these neurons are indeed *Atoh1* dependent (Imondi et al., 2007). Second, given that many spinal relay tracts are restricted to specific levels along the rostral-caudal axis, it is unknown whether DI1 interneurons are generated in a similar fashion. Third, although expansion of the DP2 domain occurs in *Atoh1* null embryos, it is unknown whether there is an autonomous contribution by the DP1 domain to this expansion. Lastly, there is very little information pertaining to dorsal interneuron development in the mouse beyond E11.5. Therefore, we decided to conduct an extensive expression analysis of *Atoh1* throughout embryonic spinal cord development, and to study gene expression changes in its absence. Analyses using $Atoh1^{LacZ}$ and $Atoh1^{Null}$ alleles in combination with in situ hybridization revealed at least three migratory streams that arise from *Atoh1* dependent progenitors in the DP1 domain and that correspond to the cell bodies of the various SCT divisions. We also found that postmigratory DP1 derived cells coexpress LHX1/5 in addition to *Lhx2* and *Lhx9*, implying that a combination of *Lhx* gene expression denotes the maturation status of DI1 interneurons. In the absence of *Atoh1* and in addition to the resulting expansion of the DP2 domain, a subset of DP1 progenitors express DI2 associated homeodomain transcription factors. Finally, we show that between E13.5–E14.5 as the central canal recedes and the roof plate retracts, we detect *Atoh1*-expressing progenitors at the dorsal midline that migrate and/or project toward the overlying epithelium, thereby defining a novel population of *Atoh1*-expressing progenitors.

Materials and Methods

Mouse Strains, Timed matings, and Genotyping

Animals used in this study were previously described (Ben-Arie et al., 1997, Ben-Arie et al., 2000). Mice carrying the $Atoh1^{LacZ}$ allele were backcrossed to at least 10 generations (C57B6J) and those carrying the $Atoh^{-}$ allele up to four. Females were grouped (4–5 per cage) to synchronize estrous cycles. In the early evening, two 8–16 week-old females were placed with a singly-housed male; the presence of a vaginal plug on the following morning designated embryonic day 0.5 (E0.5). Pregnant females carrying litters staged between E11.5 and E18.5 were euthanized and uterine walls were collected and placed in ice-cold Phosphate buffered saline (PBS). Embryos were individually removed, and yolk sacs obtained for PCR-based genotyping using primers as described (Wang et al., 2005). Animal housing, husbandry, and euthanasia were conducted under guidelines of the Center for Comparative Medicine, Baylor College of Medicine.

Xgal staining

Embryos prepared for Xgal staining were harvested, rinsed, and fixed in 10% formalin for 3–20 min on ice. In some cases, back skin was removed on older-staged specimens to allow better penetration of solutions. Embryos were washed 3×10 min and pre-incubated with Xgal buffer (0.02% NP-40, 0.01% Sodium Deoxycholate, 5mM Potassium Ferricyanide, 5 mM Potassium Ferrocyanide, in 1x PBS) for 15 min at RT in the dark, then incubated with Xgal buffer containing 1 mg/ml Xgal (Gold Biotechnology). After an 18–24 h incubation at 37°C in the dark, specimens were washed 3×10 min (PBS), post-fixed overnight at 4°C, washed again and stored in 70% ethanol at 4°C prior to paraffin-embedded sectioning (10 μm), which has been described elsewhere (Ben Arie et al 2000). Slides were viewed with an Axioplan2 microscope (Zeiss, Germany), and images captured using Axiovision software (Zeiss). Images are representative of 2–3 animals per genotype at all stages.

Immunofluorescence and blinded cell quantification

Specimens used for immunofluorescent labeling were collected as described above. Embryos older than E16.5 were partially deviscerated to ensure efficient penetration of fixative within the spinal column. E11.5–E18.5 embryos were harvested and rinsed, fixed in 4% paraformaldehyde for 20–60 min on ice, washed 2×5 min then 1×2 h in cold PBS, and cryoprotected in 30% sucrose overnight at 4°C. 20–30 μm cryosections were mounted on Superfrost^{+} slides (Fisher) and stored at −20°C. On the day of the experiment, slides were thawed for 10 min, rinsed in 0.3% PBT buffer 10 min (1× PBS containing 0.3% Triton X-100), and blocked in 0.1% PBT containing 5% normal donkey serum for at least 15 min. The following primary antibodies were used: Goat anti-βGAL (AbDSerotec, 1:500); Mouse anti TUJ1 (Covance, 1:250); Mouse anti-40.2DP6/ISL1 (DSHB, 1:20); Mouse anti-4F2/LHX1/5 (DSHB, 1:20); Mouse anti-4D7/TAG1 (DSHB, 1:5); Guinea pig anti-OLIG3 (T. Muller, 1:10,000); Rabbit anti-FOXD3 (M. Goulding, 1:100); Rabbit anti-FOXP2 (Abcam, 1:1000); Rabbit anti-SOX9 (M. Wegner; Stolt et al 2003, 1:1200). Slides were incubated with primary antibody overnight at 4°C. On the following day, slides were washed 3×10 min in PBT and incubated in secondary antibody conjugated to either Cy3 (Jackson Immuno) or Alexa 488 (Invitrogen) for 2 h at 20°C. After 3×10 min washes in PBT slides were coverslipped using Vectashield (Vector Laboratories) or Prolong Gold (Invitrogen) mounting media. 24 h later, slides were sealed and viewed with a LSM510 confocal microscope and images captured using AIM software (Zeiss). Images represent data from at least three separate experiments, using 2–3 animals of each genotype at all stages. For cell quantification, images of optical sections were collected with AIM software using a 63X objective on a Zeiss 510 confocal microscope system (total magnification 630X). Data from images were projected in three dimensions and rotated using the volume rendering and display software of Osirix and compared with the original optical sections using NIH Image J. Positively stained cells from three 146 by 146 by ~18 micron regions for each numerically coded slide were manually counted and tabulated by one investigator then recoded by genotype by a second investigator who calculated summary statistics and prepared the graphs displayed in figure 6 and figure 8.

In Situ Hybridization (ISH)

Embryos were collected, rinsed, and freshly embedded for cryosectioning (20 μm). Sections were air-dried for 30 min prior to storage (−20°C). Procedures for non-radioactive ISH were described (Carson et al., 2002; Visel et al., 2004; Yaylaoglu et al., 2005) using a Tecan Genesis 200 robot (Mannedorf, Switzerland). Slides were viewed and images captured as described for Xgal staining. Images represent data from at least two separate experiments and at least two animals of each genotype at all stages assessed.

Results

Atoh1-expressing progenitors give rise to temporally and spatially distinct cell clusters that reside in the spinal intermediate gray

Drosophila ato is critical for the establishment of chordotonal organs, a mechanoreceptor embedded throughout the fly's periphery and an important proprioceptive structure (Jarman et al., 1993). Likewise, in mouse *Atoh1* has been shown to specify multiple components of the vestibular and proprioceptive systems (Bermingham et al., 2001; Machold and Fishell, 2005; Wang et al., 2005). The major proprioceptive relay at spinal levels in vertebrates is the spinocerebellar tract (SCT), which consists of both contralateral and ipsilateral projecting interneurons located in the spinal intermediate gray (Fig. S1). These projections exit the spinal cord as mossy fibers, traverse rostrally and send collaterals to the deep cerebellar nuclei, and terminate on the dendrites of cerebellar granule cells.

A number of spinocerebellar tracts have been anatomically identified (Tracey, 1995) that reside at, and receive information from, distinct regions along the rostral-caudal axis. Information from caudal positions (e.g. hindlimbs) is relayed by the ventral (vSCT) and dorsal (dSCT) subdivisions (Fig. S1A,B), whereas forelimb and neck information is carried by way of the rostral (rSCT) and cuneocerebellar (CST) subdivisions, as well as a currently unnamed subdivision (Fig. S1C,D) (Tracey, 1995). In addition, each division of the SCT is thought to be associated with transmitting different types of proprioceptive information; for instance, it has been proposed that the neurons contributing to the vSCT regulate body positioning while the dSCT is responsible for mediating fine motor control (Brodal, 1981). For clarification and as based on our observations in this study (e.g. location of cell bodies), we have designated the rostral and unnamed fiber tracts as rostral-medial, and rostral-lateral spinocerebellar tracts, respectively.

Previous work has revealed that the establishment of vSCT commissural interneurons is dependent on *Atoh1* and that βGAL(labeled *Atoh1descendents*) and DiI colocalized in both ventral and ipsilateral dorsal SCTs (Bermingham et al.,2001). To investigate whether other cell types arise from the DP1 domain, we performed an extensive analysis of *LacZ* expression driven from the *Atoh1* locus, which also allowed us to mark cells transiently beyond the time when *Atoh1* is active (Ben-Arie et al., 2000). In this study, the term wild type is used synonymously with the $Atoh1^{LacZ/+}$ genotype. Analysis of Xgal stained embryos revealed temporally and spatially distinct migratory streams. The first stream occurs between E10.5–E11.5 and consists of a medially situated population that ultimately resides in the intermediate gray; this represents the commissural interneurons of the vSCT (Fig. S2) (Bermingham et al., 2001; Helms and Johnson, 1998). By E12.5 analysis of whole mount animals revealed an additional population of cells migrating to a more lateral region of the intermediate gray (Fig. 1A–B), that is not present in *Atoh1* null mice (Fig. 1C,D, arrowheads in B,D). Unlike the medially situated population, which projects contralaterally toward the floor plate and is present along the entire length of the spinal column (Fig. 1F), the lateral population is only detected from lower cervical to hindlimb levels and does not reveal any obvious projections to the floor plate (Fig. 1H,J, arrows in H; Fig. 3). Analysis of $Atoh1^{LacZ/-}$ mice demonstrates that although many cells reside adjacent to and within the roof plate (Fig. 1G,I,K), a few cells continue to migrate and/or project to the floor plate (Fig. 1G) similar to those observed at E11.5 (Bermingham et al., 2001), though they do not take their normal residence in the intermediate gray (Fig. 1I, arrows).

We also tested for changes in gene expression using markers selected from a microarray-based screen (Miesegaes and Zoghbi, unpublished data) that label subsets of Xgal stained migratory streams. We found that *Cerebellin 2 precursor protein* (*Cbln2*) expression demarcates a stream of cells along the rostral-caudal axis of E12.5 animals (Fig. 1L,N,P). Interestingly, *Cbln2* expression was also detected in a lateral region that is only present from forelimb to hindlimb levels, and that was absent in *Atoh1* null embryos (compare Fig. 1N with Fig. 1O, arrowheads). A second gene, *SWI/SNF related, matrix associated, actin dependent regulator of chromatin, subfamily a, member 2* (*Smarca2*), was expressed in and was more specific to the lateral region of the intermediate gray (Fig. 1R,T,V). *Smarca2* was not detected in the lateral intermediate gray at E11.5 (Fig. S3), nor at E12.5 in regions rostral to the forelimbs or caudal to the hindlimbs (Fig. 1R,V). This lateral cluster of expression was no longer detectable in *Atoh1* null embryos (compare Fig. 1T with Fig. 1U, arrowheads).

Lastly, by E13.5 we detected an additional lateral population that was not present at earlier time points (Fig. 2). Xgal staining revealed a cluster of cells that was restricted to upper cervical levels (Fig. 2A, arrow). Similar to the lateral cluster observed at E12.5 that is still detectable 24 h later (Fig. 2C,E), this population does not appear to project toward the floor plate (Fig. 2A), and was completely absent in *Atoh1* null embryos (Fig. 2B,D,F, arrow in B). Like the

DP1 derived commissural interneurons (Saba et al., 2005) both lateral populations express members of the *Barh* class of homeodomain transcription factors (Fig. S4 and data not shown). Interestingly, we found that *SRY-box containing gene 6* (*Sox6*) is also expressed in a population of cells that are restricted to the upper cervical region (Fig. 2G,I,K), but was absent in *Atoh1* null embryos (compare Fig. 2G with Fig. 2H, arrowheads). *Sox6* expression was not detected at E11.5 in the area known to encompass commissural interneurons (Fig. S3). We conclude that *Cbln2* and *Smarca2* at E12.5, and *Sox6* at E13.5, serve as good markers for subsets of DP1 derived cell clusters.

Cell morphology, rostral-caudal positioning and marker analysis reveal DI1 subtype identity

Altman and Bayer performed birth dating studies in rat that aimed to address the identity and developmental origin of interneurons residing in the intermediate gray (reviewed in Altman, 2001), and identified at least two subsets of dorsally derived populations. The first population migrates from the dorsal ventricular zone to the medial region of the intermediate gray. These cells are vertically oriented and project axons ventral-medially to the floor plate where they cross to the contralateral lateral funiculus; hence, they are dorsal commissural interneurons. In contrast, the second population contains cells that are horizontally oriented and project to the ipsilateral lateral funiculus. Although the time of birth of these two cell populations remains debated, the presence of a horizontally oriented cell group has been independently confirmed (Nandi et al., 1991).

Because of this, we decided to investigate the cellular identities of the lateral vs. medial DP1 derived interneurons by evaluating their morphology and by seeking markers that might distinguish them from other cell types. Analysis of Xgal stained cross sections revealed morphological distinctions among $LacZ^+$ cells as they reached the base of the dorsal horn (Fig. 3A–H). We noticed that the longitudinal axis of cells within the medial cluster were predominantly oriented in the vertical plane (Fig. 3C), whereas those residing in the lateral cluster were in the horizontal plane (Fig. 3D). Moreover, horizontal axon bundles projecting toward and even through the adjacent lateral funiculus (lf) were clearly evident (Fig. 3D arrows). By E13.5 Xgal staining had decreased in the vertically oriented medial cell cluster but remained strong in the horizontal cluster (Fig. 3E–H), implying that they were either born later or took longer to migrate from the DP1 domain. These cells are of neuronal identity, since co-immunofluorescence experiments with neuronal class III β-Tubulin (TUJ1) reveals co-labeling of βGAL^+ cells and TUJ1 (Fig. 3I). To further investigate the nature of these neuronal cells in the lateral population and determine if they project to the floor plate, we performed co-labeling experiments with 4D7/TAG1, an axonal marker for commissural interneurons (Dodd et al., 1988). We found that axons of βGAL^+ cells corresponding to the medial cluster were labeled with TAG1 (Fig. 3J, arrow), whereas those from the laterally situated βGAL^+ cell population were not labeled with TAG1. Collectively, these data support the existence of an initial wave of DP1 derived commissural interneurons that cross contralaterally, that is followed 24h later by a stream of spatially-restricted, horizontally-oriented interneurons that project to the ipsilateral lateral funiculus. Moreover, we have identified the genetic origin, migratory path and final residence of at least some of the lateral (horizontal) cells that have been described previously using pulse-chase methods (Altman and Bayer, 1984; Nandi et al., 1991). Lastly, the restricted Xgal stained migratory streams, the gene expression patterns discussed above, and the fact that these cells are lost in absence of *Atoh1* lead us to propose that each of the various SCT interneurons are derived from the DP1 domain (see Fig. S1 and discussion below)

Lhx gene expression reveals the maturation status of DP1 derived migratory streams

We also investigated the relationship between the medial and lateral cell clusters and the previously-characterized DI1B and DI1A interneuron subtypes (Lee et al., 1998). DI1B and

DI1A cells arise between E9.5–E10.5 and migrate toward the base of the dorsal horn within 24h of birth. DI1B cells express *Lhx9*, DI1A cells express *Lhx2*, and both are dependent on *Atoh1* (Bermingham et al., 2001; Helms and Johnson, 1998; Lee et al., 1998). To determine whether these cells reside in one or more of the interneuron populations that we observed at lumbar levels, we performed a time course analysis of *Lhx* gene expression from E11.5–E15.5 (Fig. S5). As previously reported, at E11.5 most *Lhx9* expressing cells have migrated ventrally, whereas $Lhx2^{+}$ cells are at the dorsal aspect of the spinal cord. However, our analysis at later time points revealed that *Lhx2* and *Lhx9* are eventually expressed in all DP1 derived cell clusters (Fig. S5 and data not shown). Taken together, we conclude that DI1B and DI1A interneuron subtypes are intermingled within all *Atoh1* dependent DP1 derived medial and lateral cell clusters.

We next tested various interneuron markers to identify the fate of DP1 derived cells in *Atoh1* null animals at thoracic levels. We were surprised to find that at E12.5 and upon reaching the base of the dorsal horn, βGAL^{+} cells co-expressed LHX1/5 (Fig. 3K). LHX1/5 labels a variety of cell types, including DI2, DI4, DI6, and DIL^{A} interneurons (Gross et al., 2002;Muller et al., 2002). Interestingly, we did not observe $\beta GAL^{+}LHX1/5^{+}$ cells in $Atoh1^{LacZ/+}$ animals at E11.5 nor at E12.5 prior to their arrival in the intermediate gray (Fig. 3K; see also Fig. 5). βGAL did not colabel with FOXD3 (DI2 interneurons) or ISL1 (DI3 interneurons) in $Atoh1^{LacZ/+}$ mice (Fig 5G–H and Fig 3L). Thus, D1 cell types that have exited the cell cycle and have down-regulated *Atoh1* express *Lhx2/9*, whereas those that have reached the intermediate gray additionally express LHX1/5, suggesting that combinations of *Lhx* homeodomain transcription factor expression denote the maturation status of DP1 derived cell types. To determine the relationship between *Lhx1*, *Lhx2*, *Barhl2*, and *Smarca2*, we performed in situ hybridization on adjacent thoracic sections from E12.5 embryos. We found that the expression pattern of *Lhx1*, *Barhl2*, and *Smarca2* overlap in the lateral population whereas the expression domains *of Lhx2* and *Smarca2* are distinct (Fig. S6).

In the absence of Atoh1, a subset of DP1 derived cells ectopically expressess homeodomain factors and migrates to the intermediate gray

Although many cells adopt a roof plate identity in the absence of *Atoh1*, a subset continues to migrate from the DP1 domain as observed at E11.5–E12.5 (Bermingham et al., 2001). To further investigate this aberrant cell population, we decided to assess the frequency of this migration and assess the expression profile of these cells (Fig. 4, Fig 5). In thoracic sections from E12.5 embryos, we found that DP1 derived cells fail to populate the lateral cluster (Fig. 4A–B,D–E) and instead reside in a slightly ventral position (Fig. 4E arrowhead). The axons from this ectopic βGAL^{+} cluster project contralaterally across the floor plate (Fig. 4C,F) and co-label with TAG-1 (data not shown), suggesting they retain commissural interneuron properties. However, we were unable to distinguish between cells residing in what would normally become the medial cluster, and those simply migrating through that region toward the ventral location.

To discriminate between resident cells and those aberrantly in transit, we quantified the number of βGAL^{+} cells in E12.5 $Atoh1^{LacZ/+}$ and $Atoh1^{LacZ/-}$ embryos using immunofluorescence (Fig. 4G). Cells were categorized based on their location, which also reflects their developmental status: (i) cells that are most dorsal have only recently stopped dividing and are the least mature; (ii) cells in the process of migrating are further along in development and have entered the sojourn zone; and (iii) those that have completed the migratory phase have either become or are soon to become dorsal interneurons. We found that a substantial number of mutant cells migrate ventrally (73 +/− 5 cells per 30 μm at E12.5; sum of ii+iii), albeit a significantly smaller amount than that found in wild type (282 +/− 14; $p<0.01$). Altogether, about half as many cells are generated from the DP1 domain in mutant mice (129+/− 7 cells

per 30 μm as compared to 311 +/− 13 cells in wild type animals; $p<0.01$; sum of i+ii+iii). Interestingly, there was no difference between wild type and *Atoh1* null mice in the number of cells residing in the sojourn zone (ii). Moreover, under wild type conditions we found an equal distribution of cells within medial and lateral clusters (118+/− 4 per 30 μm vs. 113 +/− 5, respectively), although some were still in the process of migrating (50 +/− 5 per 30 μm). As expected, in Atoh1 null animals a significant loss of cells in both clusters was observed. We conclude that in *Atoh1* null mice the proper cell clusters fail to become established. It is likely that the few cells detected in the medial cluster are in the process of migrating ventrally rather than being settled and fully differentiated.

Next, we evaluated the expression profiles of migrating DP1 derived cells and found differences in wild type vs. *Atoh1* null embryos (Fig. 5). Past studies have shown that although DP1–DP3 progenitors exist within distinct, nonoverlapping domains of bHLH expression, the location of their boundaries can be modulated; for instance, there is an expansion of the DP2 marker *Ngn1* in E11.5 embryos lacking *Atoh1* (Gowan et al., 2001). However, whether or not this is due to the autonomous expression of D2 specific genes in the D1 lineage has been discussed but never formally addressed experimentally in differentiated neurons. As previously reported we did not observe DP1 derived cells autonomously expressing *Ngn1* in *Atoh1* null specimens (Bermingham et al., 2001;Gowan et al., 2001). However, we did find βGAL^+ cells that ectopically expressed LHX1/5 (Fig. 5A–F). Since in wild type mice LHX1/5 is detected in DI1 interneurons after they have completed their migratory phase (Fig. 3K and Fig. 5C white arrow), we wanted to use a marker that is more specific to the DI2 interneuron population. FOXD3 has been previously shown to label neural crest as well as DI2 interneurons (Dottori et al., 2001;Gross et al., 2002;Labosky and Kaestner, 1998). As with LHX1/5, we detected significant co-labeling among migrating DP1 derived precursors in *Atoh1* null mice (Fig. 5G–J). In wild type mice 0.26% double-labeled cells are detected, whereas in *Atoh1* null mice 60% of the cells are double-labeled ($p<0.01$; Fig. 5G–J). We also found differential labeling with the homeodomain factor FOXP2, which has previously been identified as a marker for spinal interneurons of an unknown subtype (Shu et al., 2001). In wild type animals, FOXP2 colabels with a subset of $LHX1/5^+$ cells that are likely to be DI2 interneurons (Fig. 5K–N) but does not colabel with *Atoh1* derived (βGAL^+) cells. However, analysis of migrating cells at both dorsal and transitory (sojourn) regions reveal βGAL^+ $FOXP2^+$ double labeling in *Atoh1* null spinal cords (Fig. 5O–Z). Analysis with the DI3 interneuron marker ISL1 revealed no substantial differences between genotypes (Bermingham et al., 2001). We conclude that in addition to an expansion of the *Ngn1* expressing DP2 domain, some *Atoh1* null DP1 derived precursors migrating from the dorsal spinal cord have adopted a DI2 commissural interneuron fate.

Identification of late-generated Atoh1 expressing cells

The presence of the non-neuronal, cap-like structure that defines the roof plate is critical to ensure proper spinal cord development. Once established, the roof plate secretes factors that are critical for the induction of DP1–DP3 progenitor domains (Lee et al., 2000). The roof plate also functions to prevent aberrant crossing of commissural axons (Augsburger et al., 1999; Butler and Dodd, 2003; McCabe and Cole, 1992; Snow, 1990), and likely plays a role in the reorganization of the spinal cord into the characteristic X-shaped structure seen in the transverse plane of adults (Altman, 2001). As we evaluated Xgal staining in $Atoh1^{LacZ/+}$ embryos at E13.5, we noted staining along the dorsal midline of both $Atoh1^{LacZ/+}$ and $Atoh1^{LacZ/-}$ embryos (Fig. 6A–D). To confirm that $Atoh1^{LacZ}$ expression is authentic in this region we performed RNA in situ hybridization. Early on and as expected, *Atoh1* RNA was detected soon after neural tube closure and was restricted to a region corresponding to the DP1 progenitor domain, located directly adjacent to the roof plate (Akazawa et al., 1995; Ben-Arie et al., 1996) (data not shown); this pattern was maintained through E12.5. However, analysis at E14.5 revealed that *Atoh1* expression later resides at the midline and in a region similar to

that of *Msx1* (Fig. 6E–F). In addition, immunofluorescent labeling revealed that βGAL$^+$ cells at the midline exhibited the stretched morphology and vertically oriented projections typical of roof plate glia (Fig. 6G–H). We tested for roof plate specific markers at this time point and found that βGAL did not colabel with MZ-15, which recognizes the proteoglycan keratin sulfate, but did overlap with another glycoprotein marker, SSEA-1 (Fig. 6I–J). Since both of these markers are known to label roof plate glia (Snow, 1990), the observed differential labeling implies that there may be more than one cell type in the roof plate at this developmental stage. We refer to *Atoh1*-expressing cells derived from within the roof plate as Dorsal Progenitors of the Midline (DPM).

Little is known about the roof plate at late developmental stages, including its transcription factor profile. We selected two genes for analysis based on their known expression patterns. The first was *Olig3*, a bHLH factor that plays an important role in spinal cord neurogenesis at earlier time points, including the generation of DI1 interneurons, and later is expressed at the dorsal midline similar to what we observed with *Atoh1* (Ding et al., 2005; Muller et al., 2005). The second was *Sox9*, an important factor during neural crest development, however later on is critical in the ventral spinal cord for driving gliogenesis (Stolt et al., 2003).

By performing antibody labeling at E14.5 we found that βGAL$^+$ cells colabeled with OLIG3 at the midline in both wild type and *Atoh1* null embryos (Fig. 7A–D), implying that *Olig3* is either upstream from, or in separate pathways to that of *Atoh1*. Labeling with SOX9 revealed many cells along the midline and central canal of E14.5 wild type animals, as well as throughout the roof plate (Fig. 7E–F). We noted that the majority of roof plate cells were labeled with SOX9, and clearly outnumbered those expressing βGAL alone or SOX9 and βGAL together (85% SOX9$^+$; 14% βGAL$^+$; 0.54% SOX9$^+$/βGAL$^+$) (Fig. 7F,M) in wild type animals. However analysis of *Atoh1* mutant embryos revealed a dramatic increase in the number of cells co-expressing SOX9 and βGAL (Fig. 7H,M). We quantified the extent of βGAL/SOX9 immunolabeling, and found that the number of SOX9$^+$ cells at the dorsal midline decreased in *Atoh1* nulls (62% +/−6% of total cells in the roof plate vs. 85% +/−7% in wild type, $p<0.01$) and correspondingly the number of βGAL$^+$/SOX9$^+$ cells had substantially increased (16% +/−2% of total cells in the roof plate vs. 0.54% +/−0.34% in wild type, $p<0.01$). A qualitative comparison of SOX9 with OLIG3 also revealed considerable overlap only in *Atoh1* null animals (compare Fig. 7J with L). Together our data imply that in the absence of *Atoh1* in the dorsal midline domain, mutant cells had altered their fate toward a SOX9 lineage. Overall, we conclude that *Atoh1* expression is maintained within two progenitor domains (DP1 and DPM) and is critical for the correct specification of multiple cell types at both early and late time points.

Discussion

Previous studies identified the *Atoh1*-expressing DP1 progenitor domain as the source for proprioceptive commissural interneurons of the spinocerebellar tract (SCT) (Bermingham et al., 2001). We have extended these findings by identifying novel cell types derived from both the DP1 progenitor domain and within the roof plate (RP). Moreover, in addition to DP1 progenitors adopting a RP fate in absence of *Atoh1* (Bermingham et al., 2001), we report other fate switch events in the absence of *Atoh1*: the adoption of a DI2 fate in the case of DI1 interneurons as shown by the ectopic expression of LHX1/5, FOXD3, and FOXP2, and an altered fate toward a currently unknown SOX9$^+$ lineage in the case of dorsal midline (roof plate) progenitors. Additionally, we have used marker analysis to distinguish among DP1 progenitors, migrating precursors, and maturing interneurons, and we have identified genes (*Cbln2, Smarca2, Sox6*) whose expression patterns are specifically altered in *Atoh1* null embryos.

Our data reveal multiple *Atoh1*-dependent cell types arising from a common progenitor domain that reside in and project to unique regions of the spinal cord. We find that DI1B and DI1A interneurons comprise subsets of the earlier born ventrally-oriented and later born horizontally-oriented cells, whose projections we believe establish the SCT. It is interesting to note commonalities between the known subdivisions of the SCT and the various *Atoh1*-defined subpopulations we have identified. That is, the ventral subdivision (vSCT; Fig.S1A, Fig S2) is contralateral and extends the length of the spinal column; this population constitutes the medially situated commissural cells we first detect in the intermediate gray by E11.5. The dSCT (Fig. S1A) however is ipsilateral and spans from forelimb to hindlimb (Rexed, 1954). Previous work, using an *Atoh1 enhancer-tau-GFP* transgenic mouse line, has identified a neuronal cell population at E13.5, which extend their axons ispilaterally to the lateral funiculi (Imondi et al., 2007). We extend these findings by demonstrating that these cells indeed are *Atoh1* dependent (Fig. 1 and Fig 2) and can be identified by the expression of *Smarca2* (Fig. 1H,T). Together these findings suggest that these cells contribute to the dSCT. The rSCT (Fig. S1C–D) which we redefine as consisting of medial and lateral subdivisions, reside at or above the forelimbs (Oscarsson, 1973;Tracey, 1995) and as we show, express *Sox6* (Fig. 2A,G). Collectively, we propose that the anatomical positioning of DP1 derived cells may predict the specific spinocerebellar fiber tract they contribute to. It should be noted that DiI labeling experiments performed on late stage $Atoh1^{LacZ}$ mice (when all *Atoh1* dependent fiber tracts can be identified (Bermingham et al., 2001) also support this idea. Moreover, we have provided further support for the idea that *Atoh1* shares a common theme across developmental contexts; the finding that multiple temporally-distinct waves arise from a single *Atoh1*-expressing progenitor pool in the spinal cord is an event that also occurs in the rhombic lip, the cochlea, and the intestine (Chen et al., 2002;Machold and Fishell, 2005;Wang et al., 2005;Yang et al., 2001). Curiously, spinal cord DI1 interneurons are now the second population, along with motor neurons, that have been found in regionally restricted positions along the rostral-caudal axis (Hollyday and Hamburger, 1977).

Through analysis of known interneuron markers we reveal a novel relationship between the DI1 cell population and LHX1/5, a marker that is typically used to delineate other dorsal interneuron subtypes (Fig. 8). *Lhx1* and *Lhx5* do not appear to have a direct role in cell specification but rather are important for maintaining inhibitory cell identity (Pillai et al., 2007;Zhao et al., 2007). Although dorsal interneurons are considered glutamatergic (Cheng et al., 2005), *Lhx1* is expressed in enteroendocrine cells, an *Atoh1*-dependent cell type in the developing and adult gut (Larsson et al., 1995). We propose that spinal cord precursors that have just exited the cell cycle, have begun or are in the process of migrating, and have down regulated *Atoh1* can be identified by the expression of *Lhx2/9* (Fig. 8A–B,Fig S5). At E12.5 the migrating $Lhx2/9^{+}$ cell cluster divides into a vertical and a horizontal oriented cell cluster, which was recently confirmed by Wilson and colleagues (Wilson et al., 2008). Using marker analysis in this study we can discriminate between the contralateral projecting ($TAG1^{+}$) and ipsilateral projecting ($Smarca2^{+}$) cell clusters (Fig. 8C). Postmigratory DP1 derived interneurons that have reached the intermediate gray and are presumably more mature additionally express *Lhx1/5* (Fig. 8C).

What happens to the fate of spinal cord progenitors in the absence of *Atoh1*? Other than in the external granule layer of the cerebellum, progenitors are still generated in *Atoh1* null animals. It therefore seems likely that *Atoh1* plays a role in driving cells away from a mitotic program and toward a specific cell lineage. Gain-of-function studies have provided some support for this hypothesis (Helms et al., 2001; Zheng and Gao, 2000). Still, although DP1 and Dorsal Progenitors of the Midline (DPM) cells in *Atoh1* null mice may have failed to differentiate and have accumulated at the midline, a significant number have adopted alternative identities. In the case of DI1 interneurons, cells have adopted either a roof plate or a DI2 interneuron fate (Fig. 5 and Fig 7). We note that past studies do not indicate any significant alteration in

proliferation or cell death in the spinal cord (Bermingham et al., 2001). In addition, there is also no significant decrease in migrating cells in the sojourn zone in *Atoh1* null animals at E11.5 (data not shown). Moreover, as we and others have not observed direct colocalization of βGAL and a DP2 progenitor marker in *Atoh1* null animals (Bermingham et al., 2001; Gowan et al., 2001), it is likely that the observed fate switch results from a lack of repression rather than direct activation of a DI2 interneuron program. With regard to the DPM population, we observed a dramatic alteration in the number of $\beta GAL^{+}SOX9^{+}$ cells at the midline, suggesting a failure of $Atoh1^{-}$ DPM cells to repress SOX9. Unlike DP1 progenitors that are induced by factors from within the roof plate, the source of $Atoh1^{+}$ DPM progenitors is currently unknown. It remains elusive as to whether they are generated de novo, asymmetrically from a common mother cell to that of a $Sox9^{+}$ cell, or directly from the $SOX9^{+}$ population (rapidly inactivating *Sox9* in the process), although studies on *Sox* factors in the inner ear suggest the latter to be a likely scenario (Kiernan et al., 2005; Saint-Germain et al., 2004).

Finally, our data reveal novel marker gene expression, which can be used to identify the different *Atoh1* derived subpopulations. We identified *Smarca2* as a marker for a lateral cluster of cells present from forelimb to hindlimb. *Smarca2* is a member of the *Trithorax* group of homeotic gene regulators that closely resembles SWI2/SNF2 in budding yeast (Tamkun et al., 1992) and may play a role in peripheral nervous system development (Elfring et al., 1998; Reyes et al., 1998). Indeed, cell type specific chromatin remodeling complexes have been found in the developing nervous system (Olave et al., 2002), and the exchange of subunits within them plays a critical role in regulating the proliferative status of neuronal progenitors (Lessard et al., 2007). In addition, the pattern of *Sox6* expression implicates the presence of a rostrally-restricted cell population, similar to our findings in Xgal stained $Atoh1^{LacZ/+}$ embryos. Interestingly, studies of motor column neurons have revealed gene expression patterns that also reflect regionalized cell types (Belting et al., 1998; de la Cruz et al., 1999). Further studies will be required to address the exact nature of how these and other genes influence neuronal development in the spinal cord.

Supplementary Material

Refer to Web version on PubMed Central for supplementary material.

Acknowledgments

We would like to thank B. Antalfy and members of the BCM microarray and in situ hybridization core facilities for technical assistance, M. Strivens for technical commentary regarding diagram generation, and S. Lee and members of the Zoghbi laboratory for insightful commentary on the manuscript. Special thanks to T. Jessell's laboratory for advice and valuable reagents. This work was funded by HHMI and the BCM Gene Expression Core (MRDDRC-NIH grant HD02464).

References

Akazawa C, Ishibashi M, Shimizu C, Nakanishi S, Kageyama R. A mammalian helix-loop-helix factor structurally related to the product of Drosophila proneural gene atonal is a positive transcriptional regulator expressed in the developing nervous system. J Biol Chem 1995;270:8730–8738. [PubMed: 7721778]

Altman J, Bayer SA. The development of the rat spinal cord. Adv Anat Embryol Cell Biol 1984;85:1–164. [PubMed: 6741688]

Altman, J.; Bayer, SA. Development of the Human Spinal Cord: an Interpretation Based on Experimental Studies in Animals. New York: Oxford University Press; 2001.

Augsburger A, Schuchardt A, Hoskins S, Dodd J, Butler S. BMPs as mediators of roof plate repulsion of commissural neurons. Neuron 1999;24:127–141. [PubMed: 10677032]

Belting HG, Shashikant CS, Ruddle FH. Multiple phases of expression and regulation of mouse Hoxc8 during early embryogenesis. J Exp Zool 1998;282:196–222. [PubMed: 9723177]

Ben-Arie N, Hassan BA, Bermingham NA, Malicki DM, Armstrong D, Matzuk M, Bellen HJ, Zoghbi HY. Functional conservation of atonal and Math1 in the CNS and PNS. Development 2000;127:1039–1048. [PubMed: 10662643]

Ben-Arie N, Bellen HJ, Armstrong DL, McCall AE, Gordadze PR, Guo Q, Matzuk MM, Zoghbi HY. Math1 is essential for genesis of cerebellar granule neurons. Nature 1997;390:169–172. [PubMed: 9367153]

Ben-Arie N, McCall AE, Berkman S, Eichele G, Bellen HJ, Zoghbi HY. Evolutionary conservation of sequence and expression of the bHLH protein Atonal suggests a conserved role in neurogenesis. Hum Mol Genet 1996;5:1207–1216. [PubMed: 8872459]

Bermingham NA, Hassan BA, Price SD, Vollrath MA, Ben-Arie N, Eatock RA, Bellen HJ, Lysakowski A, Zoghbi HY. Math1: an essential gene for the generation of inner ear hair cells. Science 1999;284:1837–1841. [PubMed: 10364557]

Bermingham NA, Hassan BA, Wang VY, Fernandez M, Banfi S, Bellen HJ, Fritzsch B, Zoghbi HY, et al. Proprioceptor pathway development is dependent on Math1. Neuron 2001;30:411–422. [PubMed: 11395003]

Briscoe J, Pierani A, Jessell TM, Ericson J. A homeodomain protein code specifies progenitor cell identity and neuronal fate in the ventral neural tube. Cell 2000;101:435–445. [PubMed: 10830170]

Butler SJ, Dodd J. A role for BMP heterodimers in roof plate-mediated repulsion of commissural axons. Neuron 2003;38:389–401. [PubMed: 12741987]

Carson JP, Thaller C, Eichele G. A transcriptome atlas of the mouse brain at cellular resolution. Curr Opin Neurobiol 2002;12:562–565. [PubMed: 12367636]

Chen P, Johnson JE, Zoghbi HY, Segil N. The role of Math1 in inner ear development: Uncoupling the establishment of the sensory primordium from hair cell fate determination. Development 2002;129:2495–2505. [PubMed: 11973280]

Cheng L, Samad OA, Xu Y, Mizuguchi R, Luo P, Shirasawa S, Goulding M, Ma Q. Lbx1 and Tlx3 are opposing switches in determining GABAergic versus glutamatergic transmitter phenotypes. Nat Neurosci 2005;8:1510–1515. [PubMed: 16234809]

Cole, J.; Paillard, J. Living without touch and peripheral information about body position and movement: studies with deafferented subjects. In: Bermudez, J., et al., editors. The Body And The Self. Cambridge: MIT Press; 1995.

de la Cruz CC, Der-Avakian A, Spyropoulos DD, Tieu DD, Carpenter EM. Targeted disruption of Hoxd9 and Hoxd10 alters locomotor behavior, vertebral identity, and peripheral nervous system development. Dev Biol 1999;216:595–610. [PubMed: 10642795]

Ding L, Takebayashi H, Watanabe K, Ohtsuki T, Tanaka KF, Nabeshima Y, Chisaka O, Ikenaka K, Ono K. Short-term lineage analysis of dorsally derived Olig3 cells in the developing spinal cord. Dev Dyn 2005;234:622–632. [PubMed: 16145668]

Dodd J, Morton SB, Karagogeos D, Yamamoto M, Jessell TM. Spatial regulation of axonal glycoprotein expression on subsets of embryonic spinal neurons. Neuron 1988;1:105–116. [PubMed: 3272160]

Dottori M, Gross MK, Labosky P, Goulding M. The winged-helix transcription factor Foxd3 suppresses interneuron differentiation and promotes neural crest cell fate. Development 2001;128:4127–4138. [PubMed: 11684651]

Elfring LK, Daniel C, Papoulas O, Deuring R, Sarte M, Moseley S, Beek SJ, Waldrip WR, Daubresse G, DePace A, Kennison JA, Tamkun JW. Genetic analysis of brahma: the Drosophila homolog of the yeast chromatin remodeling factor SWI2/SNF2. Genetics 1998;148:251–265. [PubMed: 9475737]

Gowan K, Helms AW, Hunsaker TL, Collisson T, Ebert PJ, Odom R, Johnson JE. Crossinhibitory activities of Ngn1 and Math1 allow specification of distinct dorsal interneurons. Neuron 2001;31:219–232. [PubMed: 11502254]

Gross MK, Dottori M, Goulding M. Lbx1 specifies somatosensory association interneurons in the dorsal spinal cord. Neuron 2002;34:535–549. [PubMed: 12062038]

Helms AW, Johnson JE. Specification of dorsal spinal cord interneurons. Curr Opin Neurobiol 2003;13:42–49. [PubMed: 12593981]

Helms AW, Gowan K, Abney A, Savage T, Johnson JE. Overexpression of MATH1 disrupts the coordination of neural differentiation in cerebellum development. Mol Cell Neurosci 2001;17:671–682. [PubMed: 11312603]

Helms AW, Johnson JE. Progenitors of dorsal commissural interneurons are defined by MATH1 expression. Development 1998;125:919–928. [PubMed: 9449674]

Hollyday M, Hamburger V. An autoradiographic study of the formation of the lateral motor column in the chick embryo. Brain Res 1977;132:197–208. [PubMed: 890480]

Imondi R, Jevince AR, Helms AW, Johnson JE, Kaprielian Z. Mis-expression of L1 on pre-crossing spinal commissural axons disrupts pathfinding at the ventral midline. Mol Cell Neurosci 2007;36:462–471. [PubMed: 17884558]

Ishizuka N, Mannen H, Hongo T, Sasaki S, et al. Trajectory of group Ia afferent fibers stained with horseradish peroxidase in the lumbosacral spinal cord of the cat: three dimensional reconstructions from serial sections. J Comp Neurol 1979;186:189–211. [PubMed: 87406]

Jarman AP, Grau Y, Jan LY, Jan YN. atonal is a proneural gene that directs chordotonal organ formation in the Drosophila peripheral nervous system. Cell 1993;73:1307–1321. [PubMed: 8324823]

Kiernan AE, Pelling AL, Leung KK, Tang AS, Bell DM, Tease C, Lovell-Badge R, Steel KP, Cheah KS. Sox2 is required for sensory organ development in the mammalian inner ear. Nature 2005;434:1031–1035. [PubMed: 15846349]

Labosky PA, Kaestner KH. The winged helix transcription factor Hfh2 is expressed in neural crest and spinal cord during mouse development. Mech Dev 1998;76:185–190. [PubMed: 9767163]

Larsson L-I, Tingstedt J-E, Madsen OD, Serup P, Hougaard DM. The LIM-homeodomain protein Isl-1 segregates with somatostatin but not with gastrin expression during differentiation of somatostatin/gastrin precursor cells. Endocrine 1995;3:519–524.

Lee KJ, Dietrich P, Jessell TM. Genetic ablation reveals that the roof plate is essential for dorsal interneuron specification. Nature 2000;403:734–740. [PubMed: 10693795]

Lee KJ, Mendelsohn M, Jessell TM. Neuronal patterning by BMPs: a requirement for GDF7 in the generation of a discrete class of commissural interneurons in the mouse spinal cord. Genes Dev 1998;12:3394–3407. [PubMed: 9808626]

Lessard J, Wu JI, Ranish JA, Wan M, Winslow MM, Staahl BT, Wu H, Aebersold R, Graef IA, Crabtree GR. An essential switch in subunit composition of a chromatin remodeling complex during neural development. Neuron 2007;55:201–215. [PubMed: 17640523]

Machold R, Fishell G. Math1 is expressed in temporally discrete pools of cerebellar rhombic-lip neural progenitors. Neuron 2005;48:17–24. [PubMed: 16202705]

McCabe CF, Cole GJ. Expression of the barrier-associated proteins EAP-300 and claustrin in the developing central nervous system. Brain Res Dev Brain Res 1992;70:9–24.

Millonig JH, Millen KJ, Hatten ME. The mouse Dreher gene Lmx1a controls formation of the roof plate in the vertebrate CNS. Nature 2000;403:764–769. [PubMed: 10693804]

Muller T, Anlag K, Wildner H, Britsch S, Treier M, Birchmeier C. The bHLH factor Olig3 coordinates the specification of dorsal neurons in the spinal cord. Genes Dev 2005;19:733–743. [PubMed: 15769945]

Muller T, Brohmann H, Pierani A, Heppenstall PA, Lewin GR, Jessell TM, Birchmeier C. The homeodomain factor lbx1 distinguishes two major programs of neuronal differentiation in the dorsal spinal cord. Neuron 2002;34:551–562. [PubMed: 12062039]

Muroyama Y, Fujihara M, Ikeya M, Kondoh H, Takada S. Wnt signaling plays an essential role in neuronal specification of the dorsal spinal cord. Genes Dev 2002;16:548–553. [PubMed: 11877374]

Nandi KN, Knight DS, Beal JA. Neurogenesis of ascending supraspinal projection neurons: ipsi- versus contralateral projections. Neurosci Lett 1991;131:8–12. [PubMed: 1791983]

Olave IA, Reck-Peterson SL, Crabtree GR. Nuclear actin and actin-related proteins in chromatin remodeling. Annu Rev Biochem 2002;71:755–781. [PubMed: 12045110]

Oscarsson, O. Functional organization of spinocerebellar paths. In: Iggo, A., editor. Handbook of Sensory Physiology. Vol. Vol. 2. New York: Springer; 1973.

Paillard, J. Body schema and body image: A double dissociation in deafferented patients. In: Gantchev, GN., et al., editors. Motor Control, Today and Tomorrow. Academic Publishing House: Sofia; 1999.

Pillai A, Mansouri A, Behringer R, Westphal H, Goulding M. Lhx1 and Lhx5 maintain the inhibitory-neurotransmitter status of interneurons in the dorsal spinal cord. Development 2007;134:357–366. [PubMed: 17166926]

Rexed B. A cytoarchitectonic atlas of the spinal cord in the cat. J Comp Neurol 1954;100:297–379. [PubMed: 13163236]

Reyes JC, Barra J, Muchardt C, Camus A, Babinet C, Yaniv M. Altered control of cellular proliferation in the absence of mammalian brahma (SNF2alpha). EMBO J 1998;17:6979–6991. [PubMed: 9843504]

Saba R, Johnson JE, Saito T. Commissural neuron identity is specified by a homeodomain protein, Mbh1, that is directly downstream of Math1. Development 2005;132:2147–2155. [PubMed: 15788459]

Saint-Germain N, Lee YH, Zhang Y, Sargent TD, Saint-Jeannet JP. Specification of the otic placode depends on Sox9 function in Xenopus. Development 2004;131:1755–1763. [PubMed: 15084460]

Scheibel ME, Scheibel AB. Terminal patterns in cat spinal cord. 3. Primary afferent collaterals. Brain Res 1969;13:417–443. [PubMed: 5772431]

Sherrington, C. The integrative action of the nervous system. New Haven: Yale University Press; 1906.

Shu W, Yang H, Zhang L, Lu MM, Morrisey EE. Characterization of a new subfamily of winged-helix/forkhead (Fox) genes that are expressed in the lung and act as transcriptional repressors. J Biol Chem 2001;276:27488–27497. [PubMed: 11358962]

Snow DM, Steindler DA, Silver J. Molecular and cellular characterization of the glial roof plate of the spinal cord and optic tectum: a possible role for a proteoglycan in the development of an axon barrier. Dev Biol 1990;138:359–376. [PubMed: 1690673]

Stolt CC, Lommes P, Sock E, Chaboissier MC, Schedl A, Wegner M. The Sox9 transcription factor determines glial fate choice in the developing spinal cord. Genes Dev 2003;17:1677–1689. [PubMed: 12842915]

Tamkun JW, Deuring R, Scott MP, Kissinger M, Pattatucci AM, Kaufman TC, Kennison JA. brahma: a regulator of Drosophila homeotic genes structurally related to the yeast transcriptional activator SNF2/SWI2. Cell 1992;68:561–572. [PubMed: 1346755]

Tracey, D. Ascending and descending pathways in the spinal cord. In: Paxinos, G., editor. The rat central nervous system. London: Academic Press; 1995.

Visel A, Thaller C, Eichele G. GenePaint.org: an atlas of gene expression patterns in the mouse embryo. Nucleic Acids Res 2004;32:D552–D556. [PubMed: 14681479]

Wang VY, Rose MF, Zoghbi HY. Math1 expression redefines the rhombic lip derivatives and reveals novel lineages within the brainstem and cerebellum. Neuron 2005;48:31–43. [PubMed: 16202707]

Wilson SI, Shafer B, Lee KJ, Dodd J. A molecular program for contralateral trajectory: Rig-1 control by LIM homeodomain transcription factors. Neuron 2008;59:413–424. [PubMed: 18701067]

Yang Q, Bermingham NA, Finegold MJ, Zoghbi HY. Requirement of Math1 for secretory cell lineage commitment in the mouse intestine. Science 2001;294:2155–2158. [PubMed: 11739954]

Yaylaoglu MB, Titmus A, Visel A, Alvarez-Bolado G, Thaller C, Eichele G. Comprehensive expression atlas of fibroblast growth factors and their receptors generated by a novel robotic in situ hybridization platform. Dev Dyn 2005;234:371–386. [PubMed: 16123981]

Zhao Y, Kwan KM, Mailloux CM, Lee WK, Grinberg A, Wurst W, Behringer RR, Westphal H. LIM-homeodomain proteins Lhx1 and Lhx5, and their cofactor Ldb1, control Purkinje cell differentiation in the developing cerebellum. Proc Natl Acad Sci U S A 2007;104:13182–13186. [PubMed: 17664423]

Zheng JL, Gao WQ. Overexpression of Math1 induces robust production of extra hair cells in postnatal rat inner ears. Nat Neurosci 2000;3:580–586. [PubMed: 10816314]

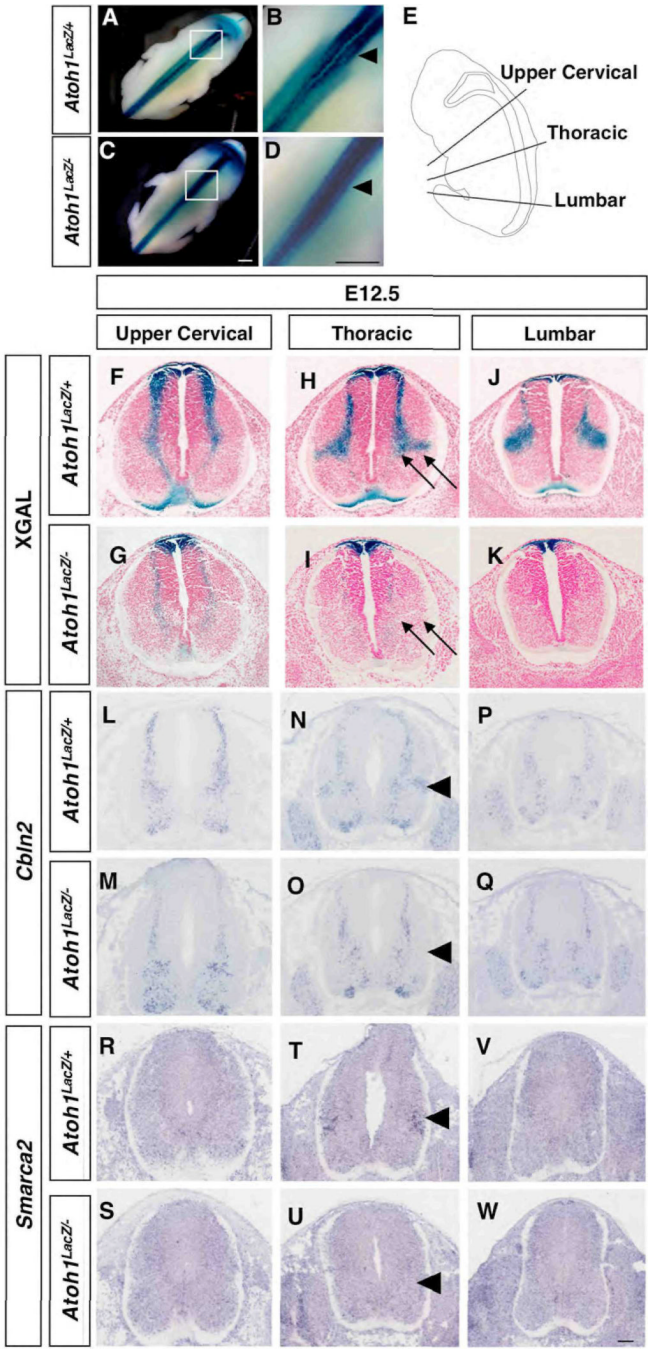

Fig. 1.

Spatially and temporally restricted migratory streams at E12.5 reflect distinct cell populations along the rostral-caudal axis. (A–D) A lateral population of Xgal-stained cells is observed in *Atoh1*$^{LacZ/+}$ (A–B) but not *Atoh1*$^{LacZ/-}$ (C–D) whole mounts beginning at lower cervical levels and extending caudally. As outlined in (E), cross sections in the transverse plane reveal spatially restricted patterns of Xgal staining and gene expression in *Atoh1*$^{LacZ/+}$ (Xgal, F–J; *Cbln2*, L–P; *Smarca2*, R–V) embryos. In *Atoh1*$^{LacZ/-}$ animals, Xgal staining is present in and around the roof plate (G–K) as well as in a subset of cells migrating ventrally. *Cbln2* (M–Q) and *Smarca2* (S–W) gene expression in a lateral cell cluster is absent in *Atoh1*$^{LacZ/-}$ mice. Scale bar: (A–D), 0.5 mm; (F–W), 50 μm.

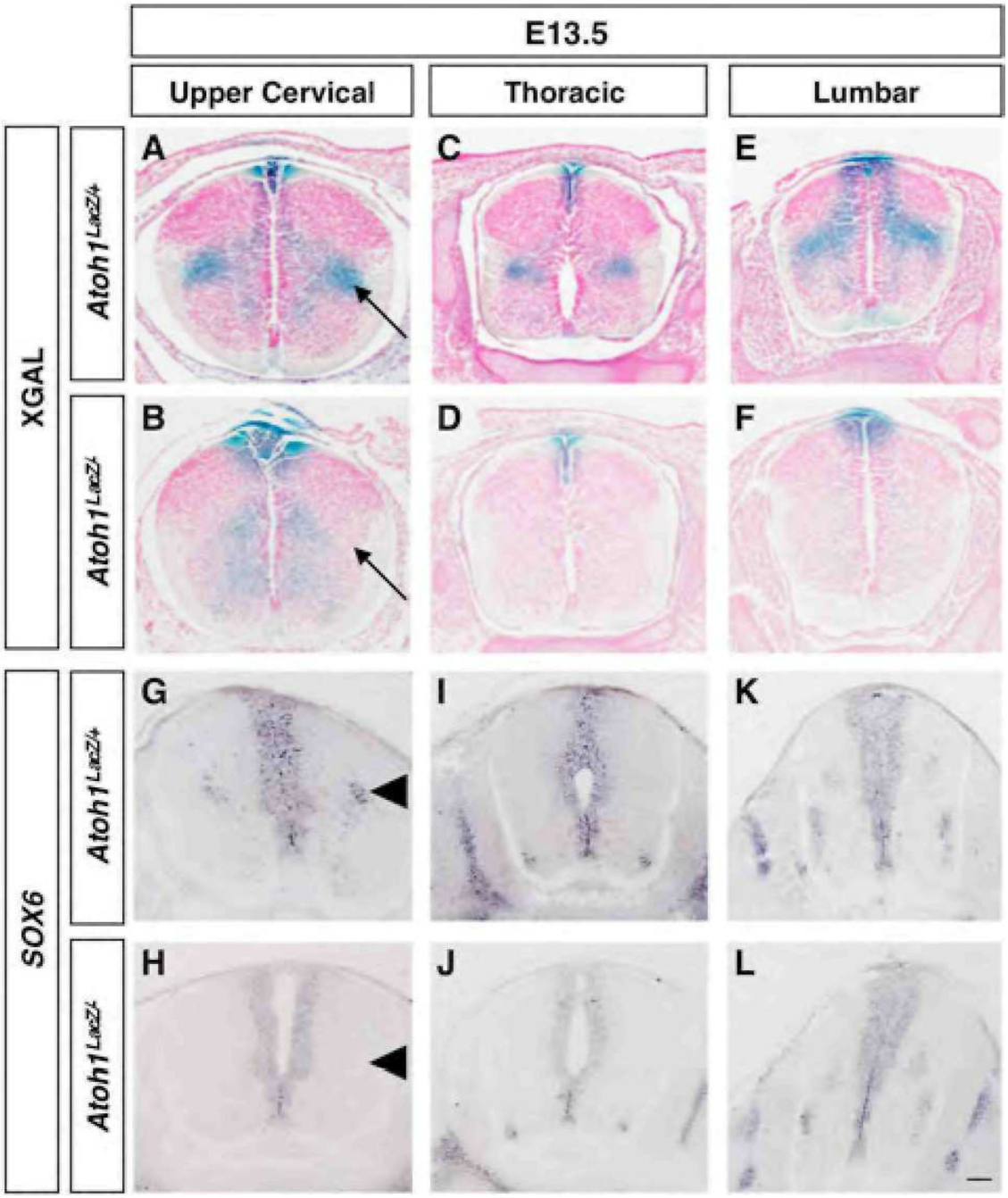

Fig. 2.

Spatially and temporally restricted migratory streams at E13.5 reflect distinct cell populations along the rostral-caudal axis. Transverse sections are as outlined in Fig. 1E. (A–F) Whereas absent at E12.5, by E13.5 a lateral population of Xgal stained cells is present in *Atoh1*$^{LacZ/+}$ (A) but not *Atoh1*$^{LacZ/-}$ (B) embryos. Analysis of *Sox6* gene expression in wild type (G–K) and *Atoh1* null (H–L) embryos reveal a similar trend. Scale bar 50 μm.

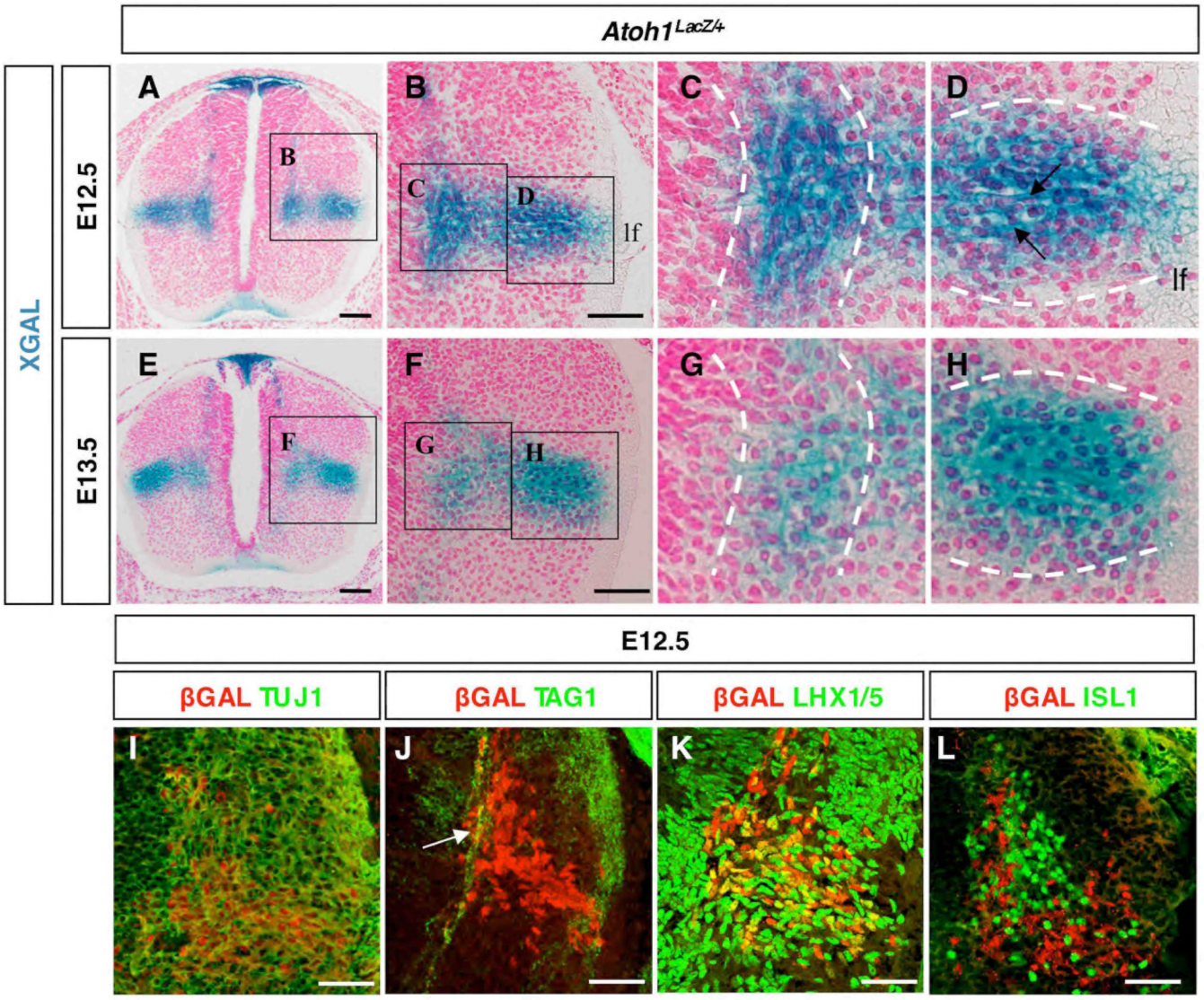

Fig. 3.

Patterns of gene expression denote maturation status and subtype identity of dorsal interneurons. Thoracic levels are shown. (A–H) Cross sections of E12.5 (A–D) and E13.5 (E-H) *Atoh1*$^{LacZ/+}$ embryos. (I–L) Subtype specification at E12.5 using βGAL and neuronal class III β-Tubulin (TUJ1, I), commissural axonal marker 4G1/TAG1 (TAG1, J), LHX1/5 (K) and ISL1 (L). Shown is the equivalent region as boxed in A. Virtually all βGAL^{+} cells are β-Tubulin positive (I), whereas only the medial population (J, arrow) and not the lateral population co-label with TAG1. As βGAL^{+} cells reach the intermediate gray they begin to express LHX1/5 (K) but not ISL1 (L). (lf) lateral funiculus. Scale bars: (A,E) 50 μm; (B,F) 25 μm; (I–L) 25 μm.

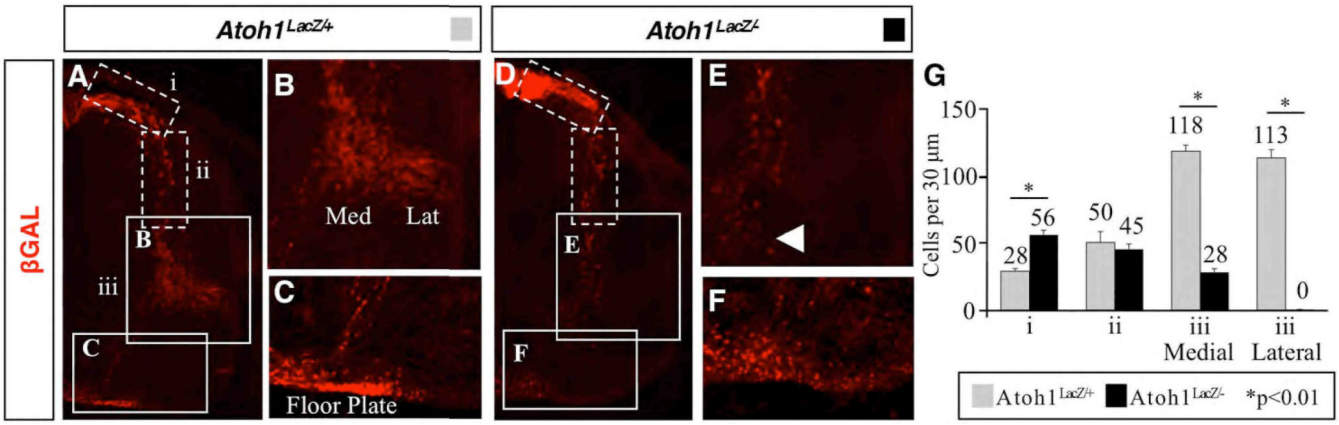

Fig. 4.

In *Atoh1* null mice, some βGAL^{+} cells continue to migrate. Forelimb-level hemisections of E12.5 *Atoh1*$^{LacZ/+}$ (A) and *Atoh1*$^{LacZ/-}$ (D) embryos, characterized as follows: Group (i) cells are dorsal-most and are the least mature; group (ii) cells are in the sojourn zone and/or are migrating ventrally through it; group (iii) cells have completed or are soon to complete migration and are beginning to settle in the intermediate gray. (B) E12.5 *Atoh1*$^{LacZ/+}$ spinal cord containing medial and lateral cell clusters. (E) In *Atoh1* null mice, the lateral cluster does not exist; cells present medially are migrating to an ectopic ventral location (arrowhead). (C,F) Axons within the floor plate of *Atoh1*$^{LacZ/+}$ (C) and *Atoh1*$^{LacZ/-}$ (F) embryos are βGAL^{+}, suggesting that mutant cells are either functioning or attempting to function as commissural interneurons. (G) Quantification of βGAL^{+} cells. There is no significant difference in the number of migrating cells between genotypes (group ii).

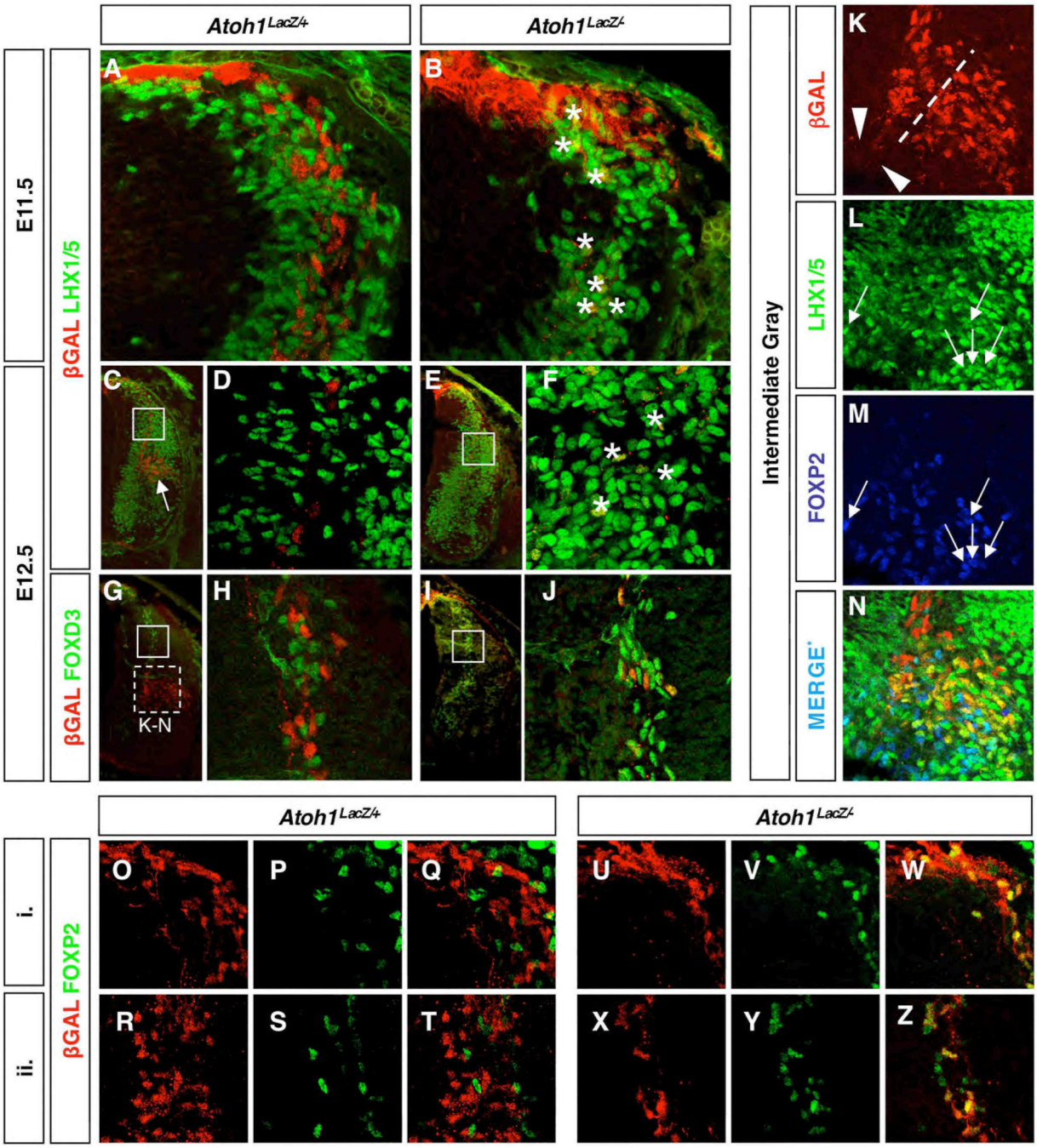

Fig. 5.

Migrating DP1 derived cells in *Atoh1* null embryos commit to a DI2 commissural interneuron fate. Thoracic levels are shown. E11.5 (A,B) and E12.5 (C–J) cross sections of *Atoh1*$^{LacZ/+}$ (A,C–D,G–H) and *Atoh1*$^{LacZ/-}$ (B,E–F,I–J) embryos immunostained for βGAL and either LHX1/5 (A–F) or FOXD3 (G–J). Asterisks are in the vicinity of double positive cells in (B) and (F). Closed boxes in (C,E,G,I) are identical to (D,F,H,J), respectively. Arrow in (C) points to the βGAL$^+$ LHX1/5$^+$ cell cluster, which is also shown in Fig. 4M. (K–N) At E12.5, subsets of LHX1/5 positive cells colabel with either βGAL or FOXP2 but never both. βGAL$^+$ axons project from the medial cluster (L, arrowheads). Area shown is depicted in (G) (dashed box). (O–Z) Analysis of E12.5 *Atoh1*$^{LacZ/+}$ (O–T), and *Atoh1*$^{LacZ/-}$ (U–Z) embryos reveal ectopic

expression of FOXP2 in *Atoh1* null mice. (O–Q) and (U–W) are representative of region (i), and (R–T) and (X–Z) of region (ii), as described in Fig. 4.

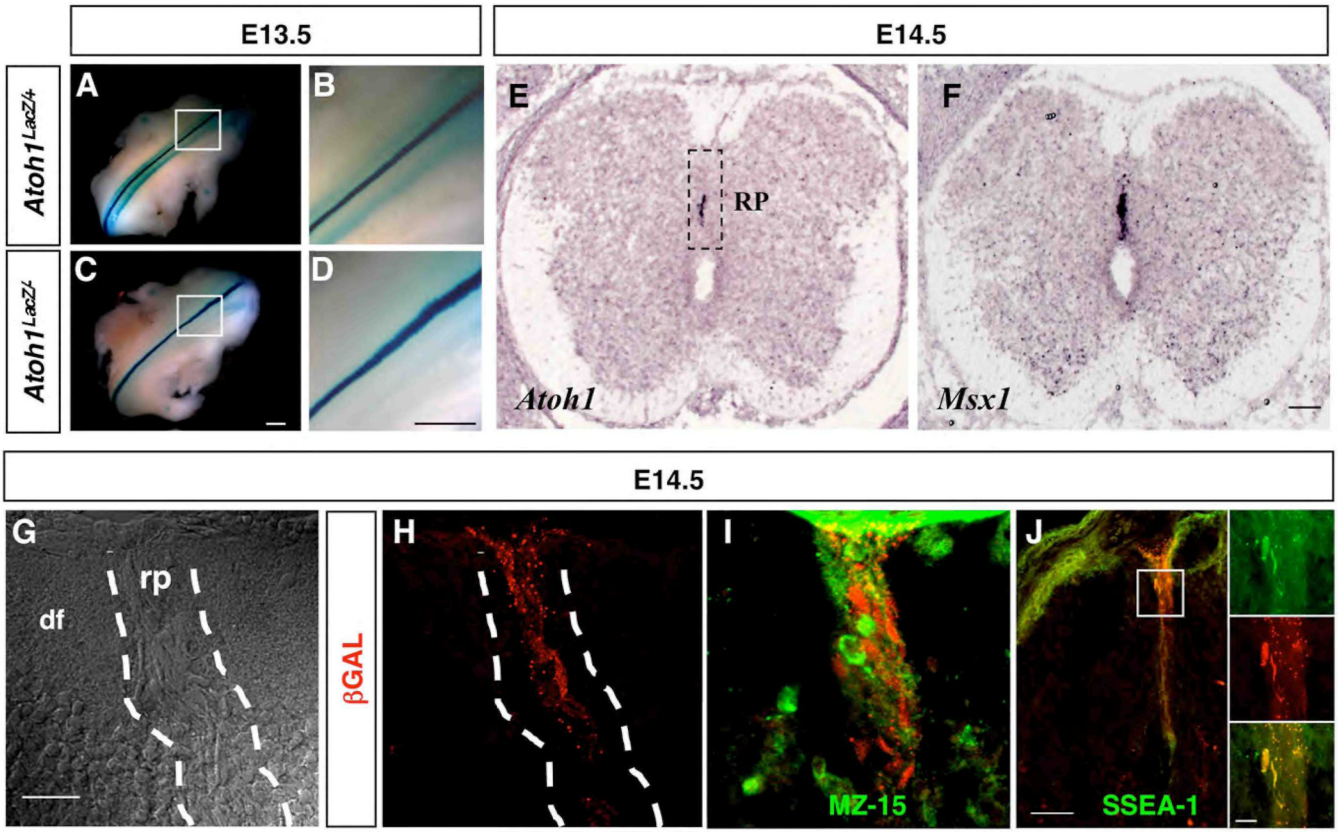

Fig. 6.

Atoh1 is expressed in a subset of roof plate glia. (A–D) Xgal-stained cells are detected at the midline of E13.5 $Atoh1^{LacZ/+}$ (A–B) and $Atoh1^{LacZ/-}$ (C–D) whole mounts, along the rostral-caudal axis. (E–F) In situ hybridization for *Atoh1* (E) and *Msx1* (F) on adjacent heterozygote forelimb level sections at E14.5 shown. Differential interference contrast image (G) of the dorsal aspect of an E14.5 $Atoh1^{LacZ/+}$ embryo, revealing cell morphology within and outside of the roof plate; βGAL^{+} cells are clearly situated in the roof plate (H). βGAL^{+} cells in the roof plate are not labeled by MZ15 (I) but do colabel with SSEA-1 (J). (rp) roof plate; (df) dorsal funiculus. Scale bars: (A–D) 0.5 mm; (E–F) 50 μm; (G–I) 50 μm; (J) 50 μm; (J inset) 25 μm.

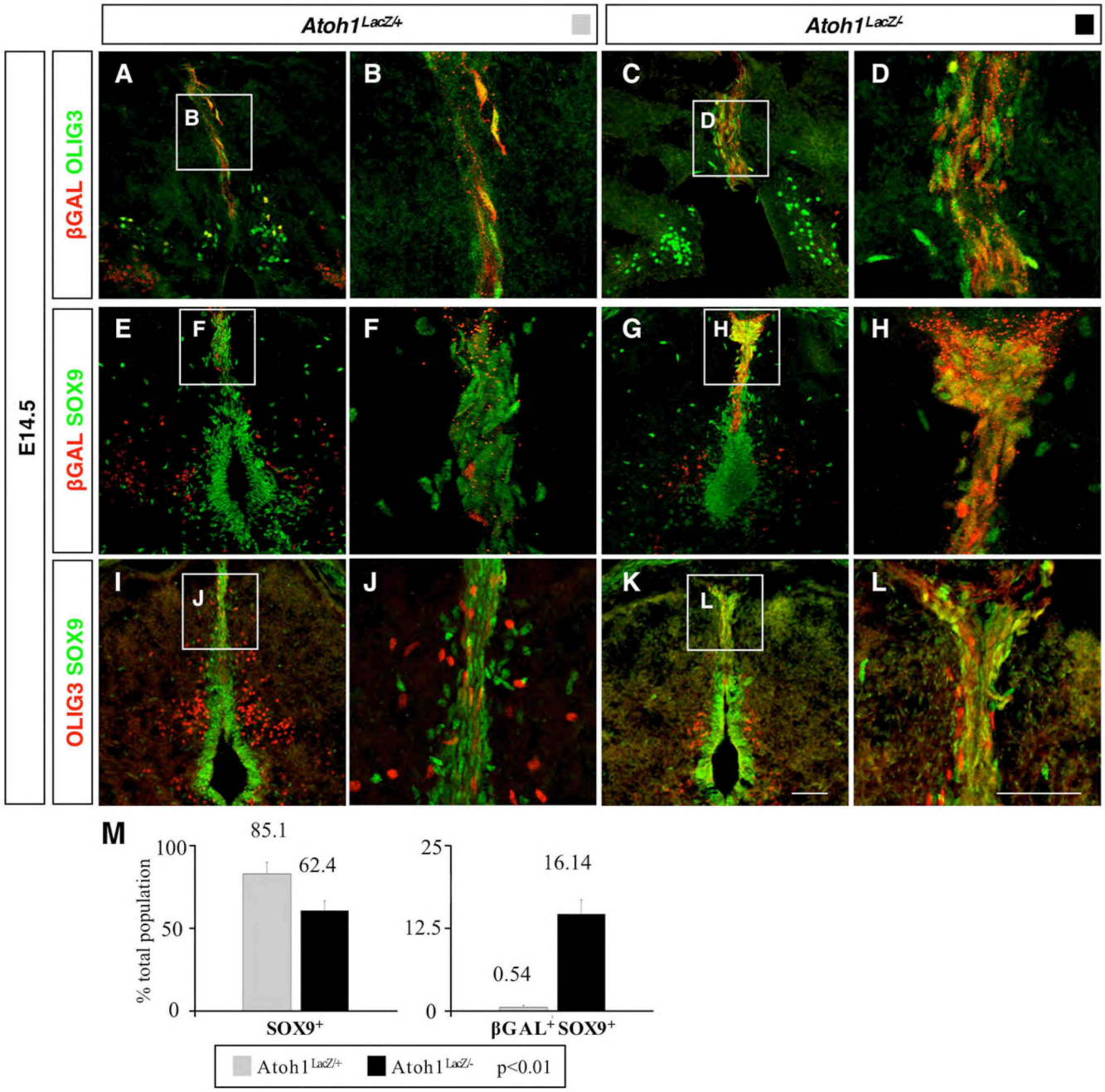

Fig. 7.

Characterization of the *Atoh1* dependent dorsal midline (DM) population. (A–D) βGAL$^+$ cells express OLIG3 (A–B), even in the absence of *Atoh1* (C–D). (E–H) βGAL$^+$ cells do not express SOX9 in *Atoh1*$^{LacZ/+}$ mice (E–F); however, there is extensive colabeling in *Atoh1* nulls (G–H). (I–L) A similar effect is observed when comparing OLIG3 and SOX9 labeling in *Atoh1*$^{LacZ/+}$ (I–J) and Atoh1$^{LacZ/-}$ (K–L) animals. (M) In *Atoh1* null mice there is a significant decrease in the number of cells that are only SOX9$^+$, but a significant increase in the number that are βGAL$^+$SOX9$^+$. Closed boxes in (A,C,E,G,I,K) are identical to (B,D,F,H,J,L), respectively. Scale bars are 50 μm.

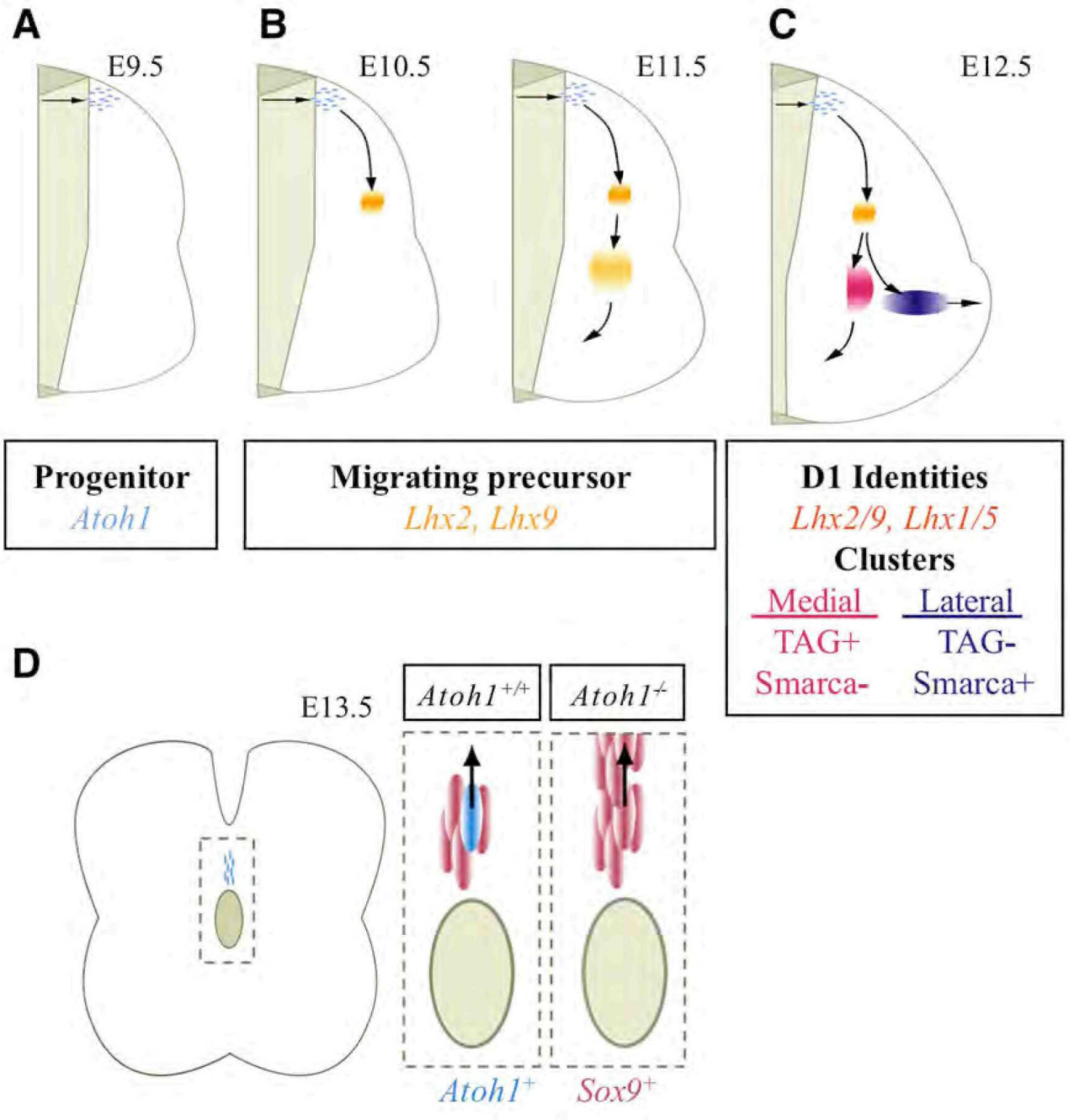

Fig. 8.

Summary of *Atoh1*-dependent cell types in the developing spinal cord, including time of migration and location along the rostral-caudal axis. DP1 progenitors express *Atoh1* (A), migrating precursors have inactivated *Atoh1* but express *Lhx2/9* (B), and in turn activate *Lhx1/5* upon arrival in the intermediate gray (C). Moreover, medial vs. lateral cell clusters may be identified by the expression of *Smarca2 and TAG*. At E13.5 a new Atoh1 progenitor domain is identified (D). Some of these cells become $SOX9^{+}$ in the absence of Atoh1. See text for details.